Journal of Alloys and Compounds, *188* (1992) 49–59
JALCOM 9007

Microstructure and thermomechanical behavior of a new class of materials: ceramic matrix composites

Jean-Louis Chermant and Moussa Gomina
Laboratoire d'Etudes et de Recherches sur les Matériaux, LERMAT, URA CNRS 1317, ISMRA, 6 Bd du M^al Juin, 14050 Caen Cedex (France)

Abstract

In this paper the main characteristics of the morphology, microstructure and mechanical properties of ceramic matrix composites are presented. Some details are also given on the processes used to produce this new class of materials and on some applications. The roles of the interfaces and of micromechanisms arising during deformation and rupture are also discussed.

1. Introduction

To develop new engines in the fields of aeronautics and space requires very high-tech materials, with specific characteristics: lightness, resistance to crack propagation, high temperatures, creep and wear, and ability to withstand use in severe environments, etc. They must be able to stand up to the problems of high speeds (see the ATSF, AGV or NASP projects), propulsion, and re-entries into the atmosphere, and have a lifetime of about 30 years. Classical metallic alloys, *i.e.* aluminum alloys, steels, superalloys, etc. cannot be used. They are now being replaced by composite materials based on Kevlar^R or carbon fibers, or by titanium or aluminum–lithium alloys. These materials have both lightness and mechanical strength.

Temperatures greater than 1273 K, and sometimes more than 2273 K, are encountered, and monolithic (or structural) ceramics can be used in the domain less than 1573–1673 K [1]. Although interest in them declined steadily between 1970 and 1980, there is currently renewed interest in for example high strength Si_3N_4, SiC or Sialon materials with very well controlled microstructure [2, 3] or nanocomposites [4]. Unfortunately, these ceramics fail in a more or less brittle manner and have low toughness. Design of the ceramic parts must be coupled with a good knowledge of the applied stress components.

To answer these problems and to provide sufficient mechanical reliability, a new class of materials has been devised: ceramic matrix composites (CMCs), *i.e.* a ceramic matrix reinforced either with ceramic particles or whiskers, or short or long ceramic fibers. The first are always brittle, but with higher strength and toughness, whereas CMCs with long ceramic fibers exhibit greater toughness owing to specific micromechanisms. The successful application of high performance composites based on ceramics—as well as on metal (see for example ref. 5) or intermetallic (see for example ref. 6) matrices—is reflected in a variety of chemical and thermomechanical properties [7]. Figure 1 presents graphs showing the interest in CMCs in the field of high temperatures [8]. In addition, these CMCs, of which carbon–carbon composites are the most developed, can also be protected by chemical vapor deposition (CVD) coatings for very high temperature applications (around 2273 K) for short periods.

If we look, for example, at the temperatures encountered by the intrados of the Hermès shuttle (Fig. 2) (which are of the same order of magnitude as those encountered by the US shuttle or the transatmospheric aircraft Orient Express), we notice that some parts of the intrados are working at temperatures greater than 1773 K [9]. The problem is then to develop appropriate materials, such as ceramic composite materials reinforced with long ceramic fibers.

This paper will focus essentially on materials made of ceramic matrices reinforced with long ceramic fibers. We give briefly some details of the elaboration processes, and we present their morphological characteristics, some mechanical properties including the role of the interfaces, and lastly some examples of uses.

2. Ceramic matrix composite processing

CMCs based on dispersed ceramic phases or on whiskers or short ceramic fibers are most often obtained by sintering in liquid (*e.g.* WC–Co cermets, Si–SiC) or solid phases (*e.g.* SiC_f–Si_3N_4, $SiO_{2,f}$–Al_2O_3, etc.).

0925-8388/92/$5.00

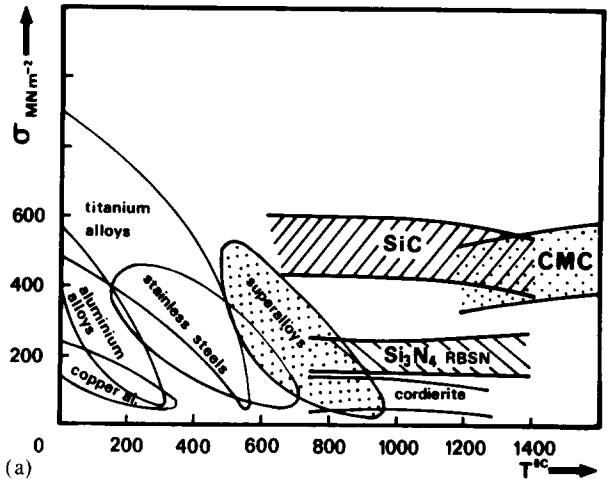

(a)

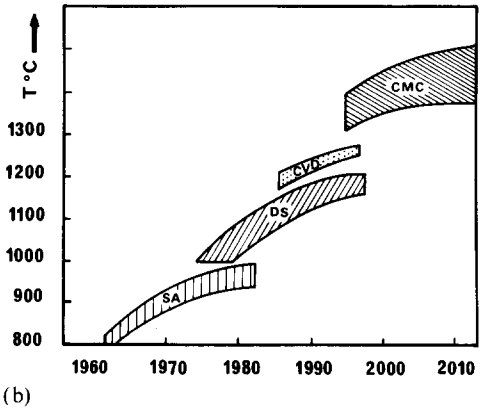

(b)

Fig. 1. Mechanical strength of different classes of materials for thermomechanical applications and their development since 1960 (SA superalloys; DS materials prepared by directional solidification; CVD materials with a chemical vapor deposition coating; CMC ceramic matrix composites). From Clark and Flemings [8].

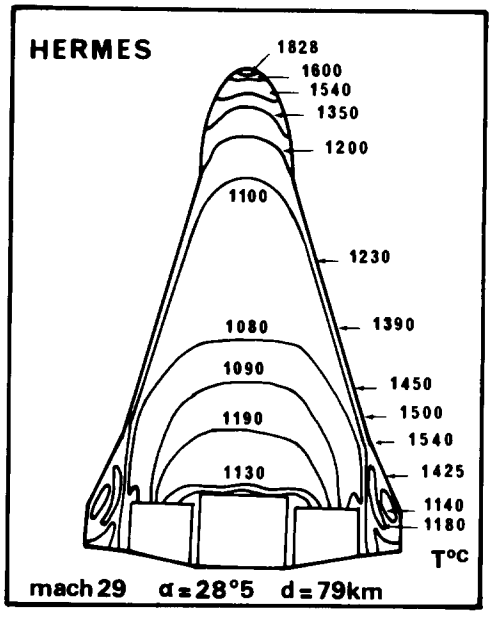

Fig. 2. Temperature distribution on the Hermès intrados for the following conditions: flight speed mach 29, altitude 79 km, angle of re-entry 28° (from a CNES document).

CMCs based on long ceramic fibers are elaborated either via a gas or liquid route. For the gas route, an impregnation preform, obtained from a multidirectional two-dimensional cloth or satin or knitting, is infiltrated by a vapor phase (chemical vapor infiltration process, CVI). Bulk infiltration requires low temperature conditions, otherwise surfaces of the pores peripheral to the part will be filled up rapidly and the infiltration will therefore be stopped. So it is necessary to control perfectly the thermodynamical parameters of the chemical reactions [10, 11]. That also explains the length of time needed to fabricate parts by this process. This process, devised in an academic institution (by the team of Professor Naslain in Bordeaux), has been developed by commercial companies (*e.g.* SEP in France, Du Pont de Nemours in the USA). It differs from CVD in the thermodynamical conditions. For CVD, high temperature conditions are required and the pores and defects on the part surface are rapidly filled up, leaving a porous internal structure, which is not the case with the CVI process. CMCs for high temperature resistance are produced by the CVI process: C_f–SiC, SiC_f–SiC (see for example materials developed by SEP, Etablissement de Bordeaux, France).

To counter the disadvantages of time and cost, one can use a liquid route. The ceramic preform is then infiltrated by a slip casting (used for short ceramic fibers in a glass matrix, *e.g.* $Nextel_f$–SiO_2) or by a polymeric solution which will give the matrix phase after polymerization, or by a sol which after drying will be transformed into a ceramic after heat treatment (*e.g.* $Al_2O_{3,f}$–Al_2O_3, SiC_f–Al_2O_3), or by a liquid phase which will infiltrate the preform with or without a chemical reaction (*e.g.* Si–SiC). For example, ONERA (Châtillon sous Bagneux, France) has developed an interesting process, now used at Aérospatiale (Etablissement de Bordeaux, France): the glass slip casting to be ceramized is pumped under vacuum through the preform of SiC fibers. SiC_f–MLAS (magnesium lithium aluminum silicate) composites are prepared by Aérospatiale using this process, followed by a hot pressing or by injection of a liquid. These processes give CMCs in a very short time and are of great economical interest [12].

3. Morphology and microstructure of ceramic matrix composites

As an illustration, Fig. 3 shows optical micrographs of some CMCs with long ceramic fibers. One notes

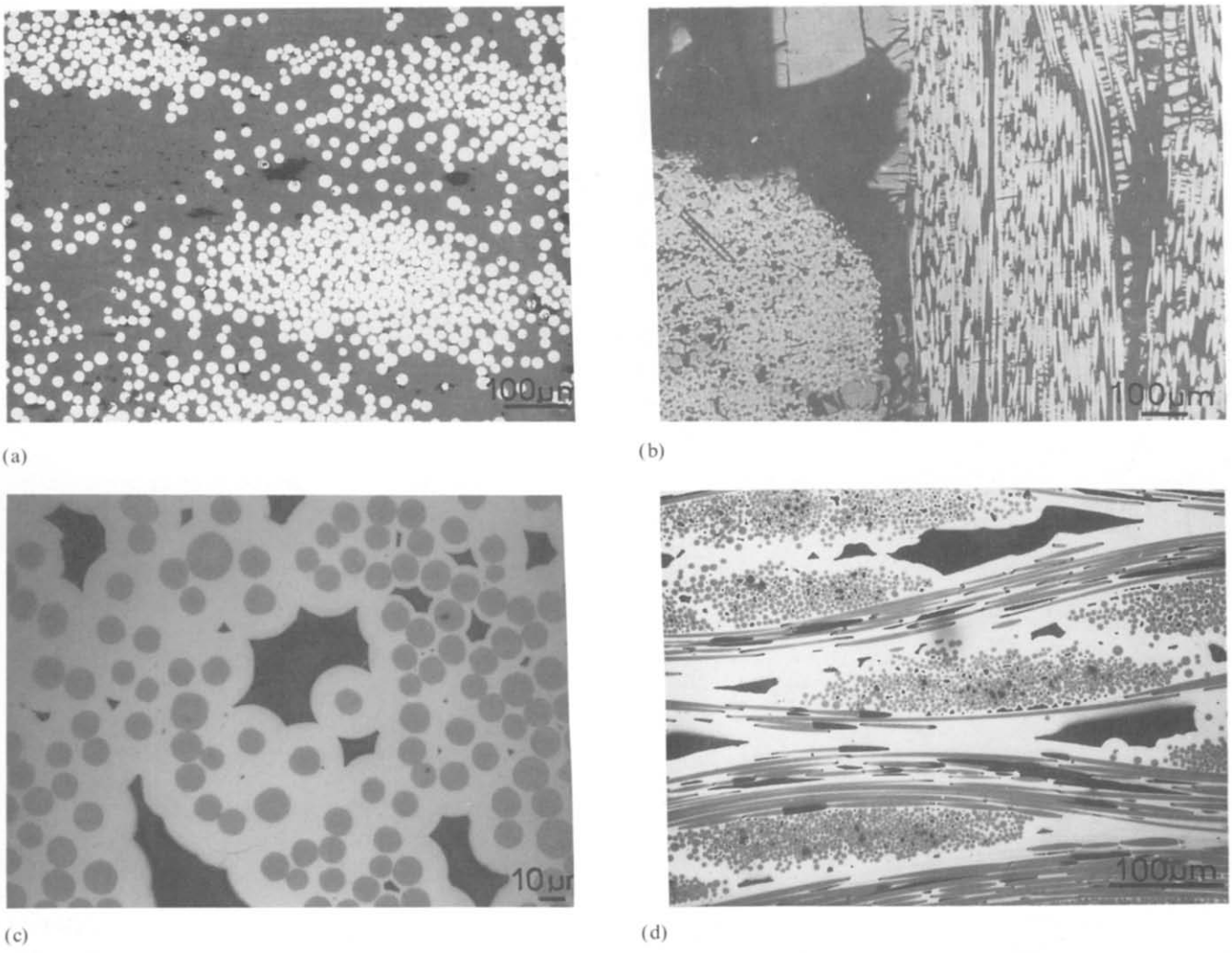

Fig. 3. Optical micrographs of different CMCs: (a) SiC_f–MLAS 1D (Aérospatiale); (b) 3D $Nextel_f$–SiO_2 (Aérospatiale); (c) C_f–SiC 2D (SEP), inside of a bundle; (d) SiC_f–SiC 2D (SEP).

always the existence of three phases at the optical microscope scale: fibers, matrix and pores.

The morphological characteristics of these three phases can be determined quantitatively using automatic image analysis techniques [13, 14]. After elimination of artefacts due to polishing and noise, it is possible using mathematical morphology [13, 15] to detect only pores or fibers, to separate the fibers in contact by a segmentation procedure, and then to carry out quantitative measurements (Fig. 4) to determine the surface area of the porosities (both small and large porosities), the mean chord length, the specific perimeter, the surface area of the fibers inside the bundles, the mean diameter of the fibers and size distribution, and the mean contact number between fibers. Experimental results for these materials are given, for example, by Abbé *et al.* [14].

Image analysis can also be used to simulate such structures in the direction perpendicular to the bundles [16]. These simulations are very useful for producing models of thermal properties or process routes.

If these materials are observed at transmission electron microscope scale, a fourth phase is observed: the interface or interphase between fibers and matrix. We will see later on the very important role played by this fourth phase, which usually governs the mechanical properties and toughness of CMCs at high temperatures. Figure 5 shows a fiber–interface–matrix sequence: one notes that the interface is complex, sometimes comprising interphase(s) and several interfaces!

4. Mechanical behavior

The interest of these materials lies in their behavior at high temperatures and in the possibility of producing planes of reinforcement oriented with regard to the stress directions encountered in service. Their behavior is very

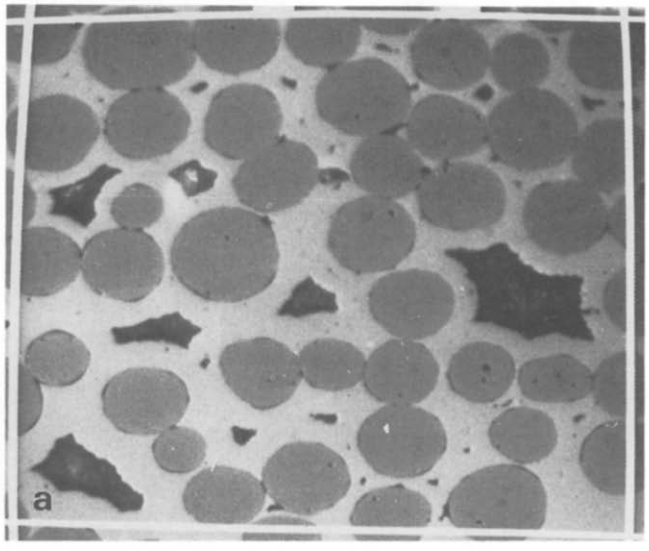

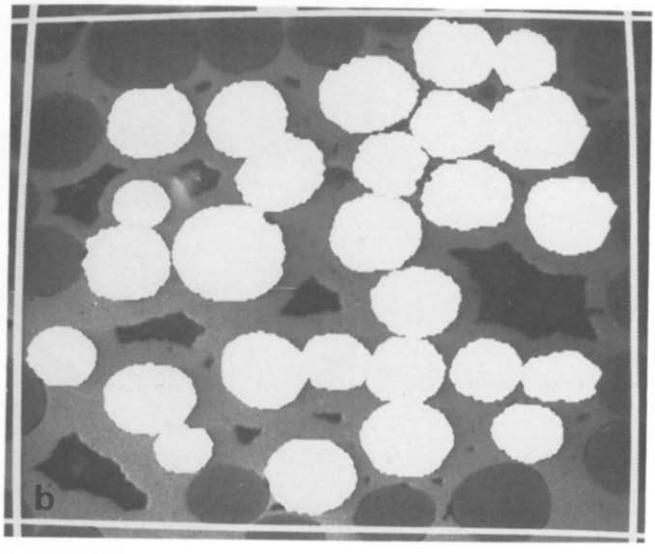

Fig. 4. Image treatment of an SiC_f–SiC composite: (a) video image; (b) final result after automatic image treatment.

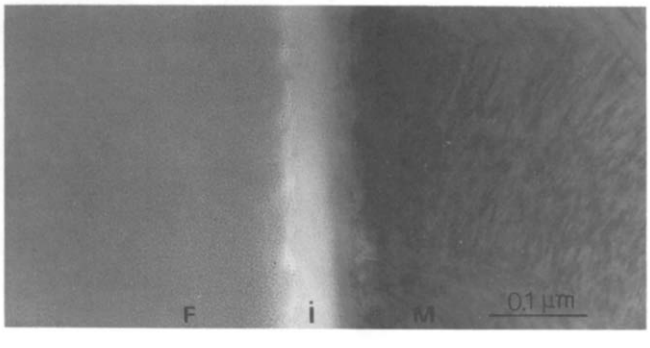

Fig. 5. Transmission electron micrograph of SiC_f–SiC (SEP) material showing the complexity of the fiber–matrix interface (FIM).

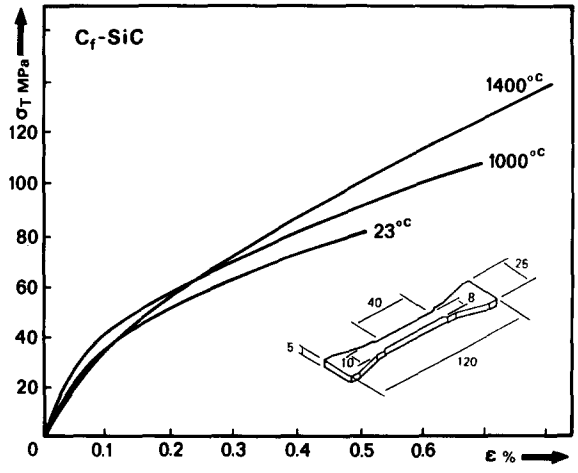

Fig. 6. Tensile curves for C_f–SiC materials (SEP) tested at different temperatures (stress σ as a function of elongation ε(%)).

specific and certain characteristics of toughness are typical of those encountered with materials of rough structures, for example siderurgical refractories, or some ceramics.... Much effort has been directed by some laboratories in France toward the study of the fracture mechanics of these materials, using macroscopic and microscopic approaches as well as ultrasonic nondestructive evaluation (see for example refs. 17–22).

These materials have very specific characteristics which we describe briefly.

During tests, in tension as well as in bending, one notes firstly that the rupture characteristics increase with temperature for C_f–SiC materials (Fig. 6), up to a certain temperature. Moreover, in the same temperature range, the linear domain is greater for SiC_f–SiC composites than for C_f–SiC composites.

Secondly, one notes that the fracture energy R absorbed during propagation of a crack a, is 50–500 times greater than that for a monolithic ceramic (Fig. 7) [23], which is one of the reasons for the interest shown in CMCs. Moreover three domains appear: the first is very small, limited by threshold stresses, corresponding to initiation of the damage; the second is very important for composites, where there is a great increase in absorbed energy due to damage; the third is where the absorbed energy decreases, owing to microcrack propagation.

Thirdly, an analysis of a loading curve (stress σ *vs.* strain ε) of a CMC (Fig. 8), shows a very small linear elastic domain characteristic of brittle materials (Fig. 8, curve a) and a "generalized plasticity" domain with residual deformation which can be more (*e.g.* SiC_f–SiC) or less (*e.g.* C_f–SiC) important. It is well known that ceramics do not show plastic behavior, at least at low temperatures. The extension of the process zone for these materials is sufficiently large to invalidate

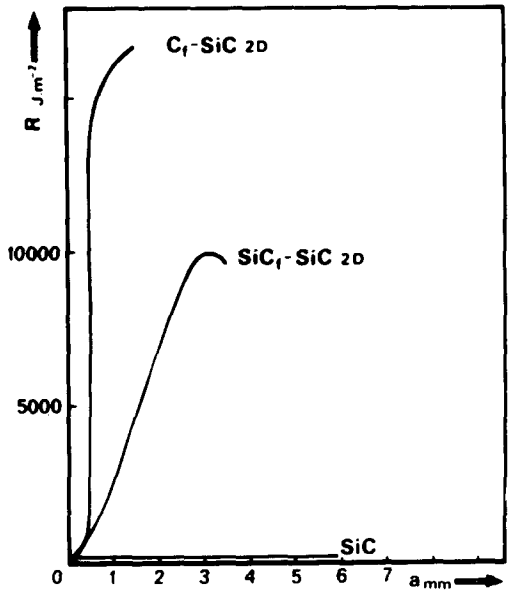

Fig. 7. Change in the rupture energy R during the propagation of a crack a for a monolithic ceramic SiC, an SiC_f–SiC 2D composite and a C_f–SiC 2D composite. From Choury [23].

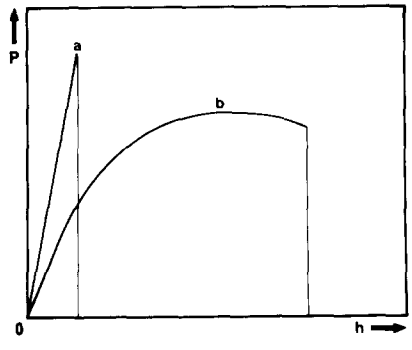

(a)

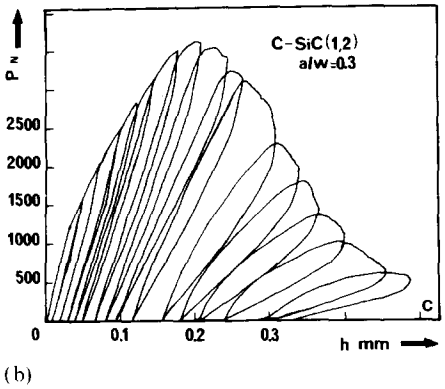

(b)

Fig. 8. Loading curves for a brittle material (curve a), a ductile material (curve b), and for a ceramic matrix composite C_f–SiC (curve c).

description of the stress and strain fields in terms of a stress intensity factor. To take into consideration these differences in behavior compared with that from linear elastic fracture mechanics (LEFM), the concepts must be adapted to non-linear fracture mechanics. The material must be considered as non-elastic: direct estimations of the parameters of the stress field (K_c for example) can be replaced by their mean values (J_c for example), which can be estimated without knowing precisely the state of the material in the neighborhood of the crack tip. Once the mean value of such a parameter is obtained, the equivalent linear elastic parameter is calculated. These methods use the J integral of Rice [24], and the methods of Garwood *et al.* [25, 26] and Sakai and coworkers [27, 28] etc. The common point of these methods is to solve the rupture of these materials in terms of crack length a. This choice allows the "perturbations" in the complementary terms to be considered depending either on the load or on the displacement [20].

For example, the semi-empirical method of Sakai is based on the energetic decomposition during loading cycles (Fig. 9). When the crack propagates from B to C, the total energy absorbed during rupture or crack resistance R is given by the surface area ABCD. If the material shows elastic behavior, then during unloading one must come back to point A. Then the surface area ABFA corresponds to the rate of release of elastic strain energy per unit surface G. It remains therefore the surface area AFBCD which takes into consideration the residual displacement ε_r and corresponds to the release rate of non-elastic energy denoted ϕ. This parameter, which corresponds to an irreversible consumption of energy, can still be called elastic energy. Therefore the fracture energy is given by

$$R = G + \phi$$

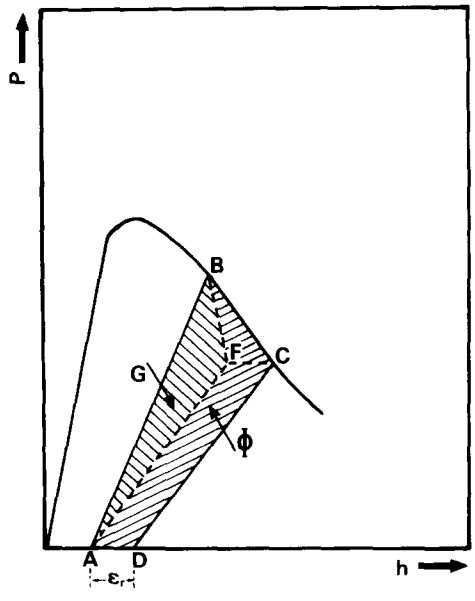

Fig. 9. Energetic decomposition during a loading cycle when the crack propagates from B to C. From Sakai *et al.* [27].

The contribution ϕ of irreversible processes to the fracture energy R will be negligible when the size of the remaining ligament to fracture becomes very small. The ratio ϕ/R will characterize the difference between ideal conditions of measurement in comparison with LEFM. It will depend on the specimen size, initial crack length, etc. [29].

If acoustic emission is used during a loading test, one obtains interesting information on the damage of these materials. This differs from one composite to another. For example, for C_f–SiC materials, damage begins when the maximum load is reached, while for SiC_f–SiC it begins at the end of the elastic domain (Fig. 10) [20, 30].

The behavior at high temperatures is obviously one of the key areas of interest, as well as the behavior as a function of time (to give predictions of creep and lifetime). Little work has been carried out in this direction [31–35]. Figure 11 shows the lifetimes of some CMCs developed by SEP Company [36].

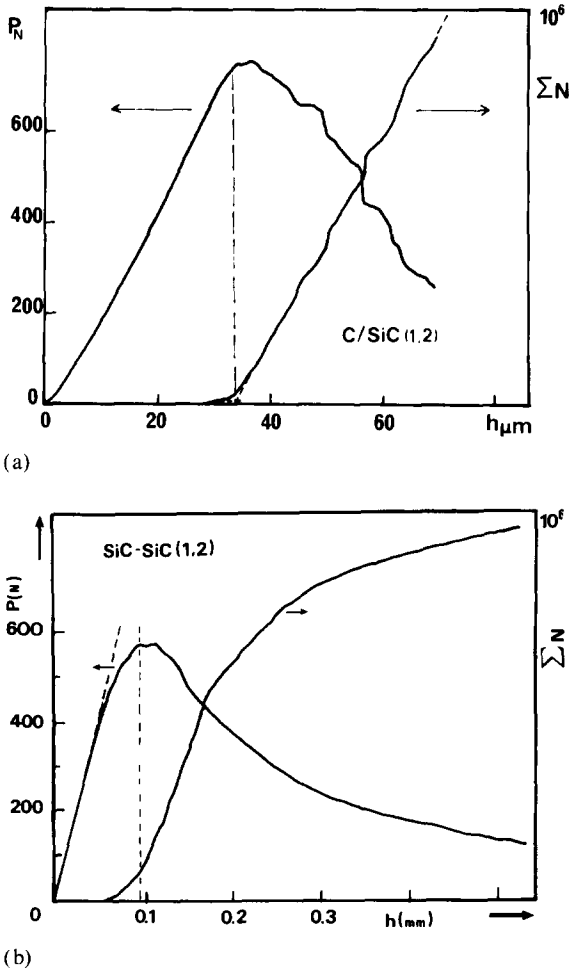

Fig. 10. Loading curve (P–h) and change in the number of events obtained from acoustic emission ΣN, for C_f–SiC and SiC_f–SiC.

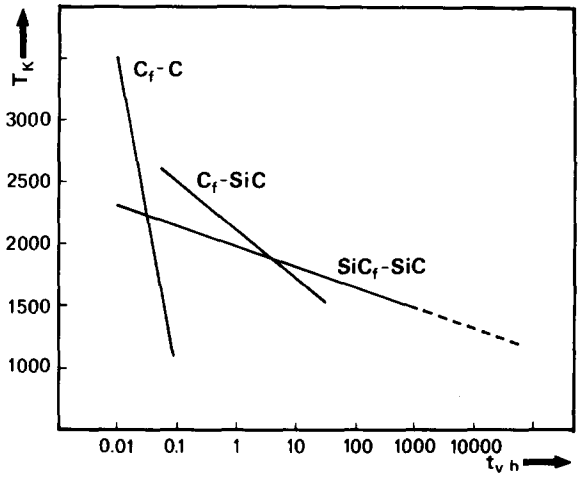

Fig. 11. Lifetime, t_v, as a function of temperature T for different CMCs: C_f–C tested under reducing atmosphere, C_f–SiC and SiC_f–SiC tested under oxidizing atmosphere. From Lamicq [36].

In addition to the macroscopic approach, it is evident that a microscopic mechanical approach is necessary. This also requires the development of specific equipment, *e.g.* micro-indentation with or without acoustic emission, *in situ* bending or tensile tests under a microscope (optical or scanning) [37–39]. This allows access to elementary mechanisms and therefore to predictions of the global behavior of these materials.

5. Interfaces and micromechanisms

It is not possible to apply fracture mechanics concepts directly to CMCs, because micromechanisms linked to the complex morphology (structure) of these materials are not taken into consideration in classical fracture energy analysis.

Fibers and pores on the one hand act or can act as crack propagation barriers: the fiber–matrix interfaces will govern the rupture and toughness of these materials [7, 40] and, locally, the mode of rupture (mode I opening or tensile mode, mode II sliding or plane shear mode). On the other hand, cracks must also be considered, at the beginning, on the atomic scale and under this condition the interfaces are to be considered as the fourth phase in which cracks can propagate if the interface is large enough (interphase) and according to its interfacial shear strength. So, when analyzing the interfacial shear strength and its thickness, many micromechanisms consuming energy will arise. They have been investigated by many authors, usually on aligned ceramic fiber composites and more especially by the team of Professor A. G. Evans at Santa Barbara (see for example refs. 7 and 41–44). Figure 12 shows some of the main micromechanisms proposed by these

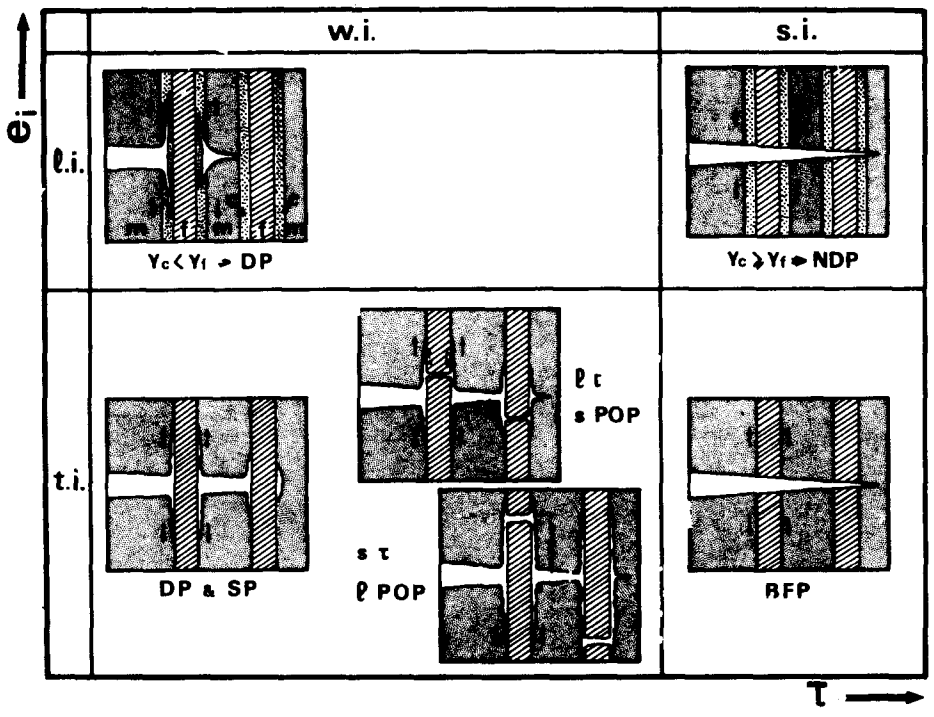

Fig. 12. Different micromechanisms arising during the deformation and fracture of CMCs as a function of the thickness of the interface e_i (l.i. large interface, t.i. thin interface) and the interfacial shear stress τ (w.i. weak interface, s.i. strong interface). DP debonding process, SP sliding process, l or s τ large or small value of τ, s or l POP small or large pull-out process, BFP brittle fracture process, NDP process without debonding.

authors. The strength of brittle material is mainly governed by three factors: the severity of pre-existent flaws, the minimum crack propagation resistance of the material in the vicinity of the flaws, and the associated magnitude of the local residual and imposed stresses [45]. We will discuss these different points.

Micromechanisms will depend essentially on the defect flaws of the ceramic fibers and on the mechanical quality and reliability of the interfaces. Different behavior will arise, owing to the existence of differences in strength due either to the process route or to the difference in expansion coefficients between fibers and matrices. Under service stress, thermomechanical stresses will be transmitted to the matrix via the fibers, through the interfaces. So if the fiber–matrix interface is strong, the crack will propagate indifferently in the matrix and through the fibers by a rectilinear (plane) route, like a brittle fracture (BFP). If the interface is weak, fiber–matrix decohesion will result (debonding process, DP), leading to pull-out (POP) which can be very important: then the broken fibers slide against the matrix and enhance the toughness by creating crack bridges which resist to crack opening [46]. If the interface is of medium quality the two phenomena will arise. So, concentrating on the physicochemical nature of the interface [47], it is possible to develop materials with strong, medium or weak interfaces, *i.e.* to produce materials which undergo more or less elongation (0.1% to more than 1%). This explains why many specific fiber coatings are tested, to develop a barrier which is not too strong, and able to deflect the cracks.

The main micromechanisms encountered in CMCs can be described briefly as follows (Fig. 12) [42, 46].

Fiber rupture from a defect flaw. The rupture does not occur at the location of maximum stress. Analysis of this process is based on classical strength distribution, which satisfies the weakest link statistics (Weibull); this allows determination of the population of fiber strength S, and of the Weibull parameter m.

Debonding and sliding processes (DP and SP). These occur when the interface is weak ($\gamma_{\text{coating}} < \gamma_f$) and thin (for example for carbon interfaces). When the interface is weak and large, debonding occurs in the interphase (DP) where the crack is deflected, and mode II rupture is present locally. A strengthened interface (greater value of the interfacial shear strength τ) leads to a small pull-out length l (POP). In fact, the material becomes more brittle as τ increases; the toughness is controlled by the sliding resistance τ which influences the pull-out length.

Flat fracture or no composite effect. If there is no debonding (NDP) with thin or thick interface, *i.e.* when

$\gamma_{coating} \approx \gamma_f$ or $\gamma_{coating} > \gamma_f$, with high value of τ (strong interface, for example SiO_2 interfaces for SiC_f–LAS materials), then there is brittle type fracture (BFP) (plane fracture) without sliding and no pull-out processes.

So, to control the toughness of such materials, it is necessary to determine the population of fiber strengths S, the Weibull parameter m, and the interfacial shear strength τ, linked to the pull-out length l. This also enables models for CMCs to be developed based on these parameters and on crack tip bridging [42, 48, 49]. The fiber–matrix interfacial shear strength can be evaluated quantitatively, and the debonding stress and pull-out can be estimated using pull-out and push-out tests [37–39, 50, 51].

In addition to the main role played by the interfaces at both room and high temperatures, we must also pay attention to the eventual physicochemical changes of the ceramic fibers with temperature when tests are performed at high temperatures. In fact ceramic fibers, except for whiskers, are not pure (from crystallographic and chemical points of view). Nicalon SiC fiber (Nippon Carbon, Japan) is partially amorphous, containing 12% oxygen; at high temperature and under stresses it crystallizes and there is diffusion of oxygen (and sometimes of carbon for certain matrices and coatings) to the interfaces. That explains why these interfaces are largely investigated by transmission electron microscopes and microprobes [47, 52].

Observation by scanning electron microscopy either of the deformed faces of CMC specimens or of the fractured surfaces provides complementary information

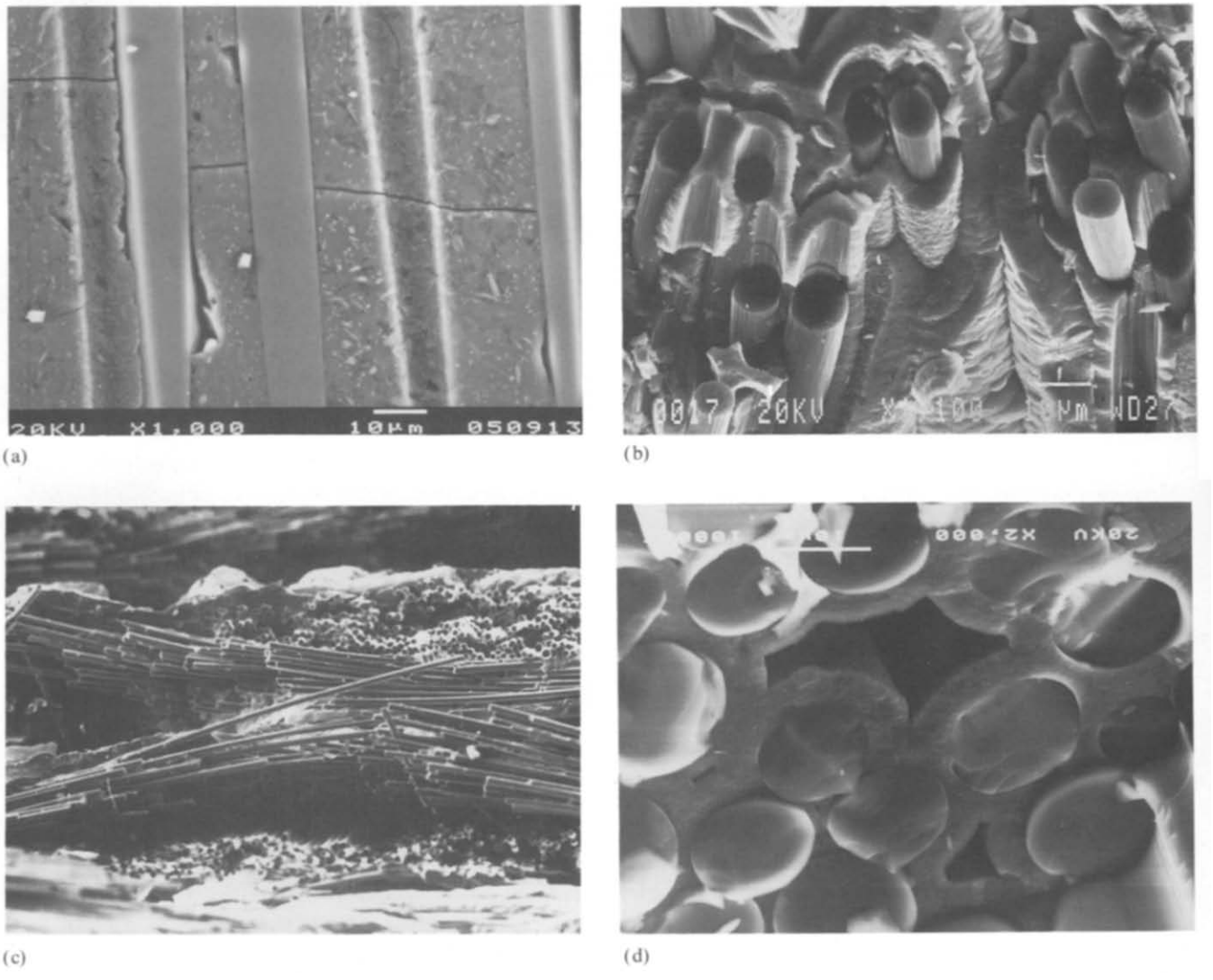

Fig. 13. Typical fracture features of CMCs: (a) microcracks in SiC_f–MLAS tested by creep at 1273 K; (b) small pull-out of C_f for C_f–SiC tested by three-point bending at 300 K; (c) large pull-out of SiC_f for SiC_f–SiC tested by three-point bending at 300 K; (d) flat fracture for SiC_f–SiC tested under air at 1273 K.

on the damage and confirms the micromechanisms proposed previously. Essentially, one observes fiber decohesion and fiber pull-out, more important for SiC fibers than for carbon fibers, matrix microcracking, and fiber fracture with or without fracture mirror. Figure 13 illustrates some typical fractographic features.

6. Ceramic matrix composite applications

Compared with the new generations of superalloys and with metallic matrix composites (MMCs), the advantages of CMCs are essentially their lightness, their temperature capability and their strength-to-weight ratio. That can be seen in Fig. 14 (from Paton [53]). CMCs are the best candidates for high temperature applications but they require stable fibers for long uses.

Figure 15 shows the change in rupture stress plotted as a function of temperature for some CMCs. It can be seen that these CMCs can effectively replace classical materials in the temperature domain between 1000 and 1600 K [54, 55].

Nevertheless, these new materials are expensive, so their main applications are in aircraft engines, rocket motors and aerospace structures. If we look at the first generation of CMCs, C_f–C, they are now used not only in these domains, but also for race cars or motorbikes and for very rapid trains (the French TGV for example).

Among the uses of C_f–SiC, SiC_f–SiC, SiC_f–MLAS, SiC_w–SiAlYON, as an illustration, one can quote the following (some of these applications are at present only experimental):

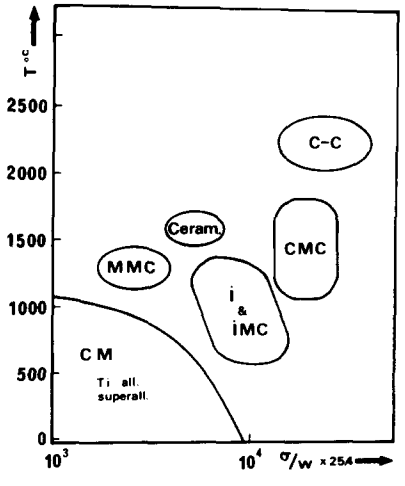

Fig. 14. Strength-to-weight ratio, σ/w, as a function of operating temperature: CM, conventional materials (titanium and superalloys); MMC, metal matrix composites; I, intermetallics; IMC, intermetallic composites; Ceram., ceramics; CMC, ceramic matrix composites; C–C, carbon–carbon composites. From Paton [53].

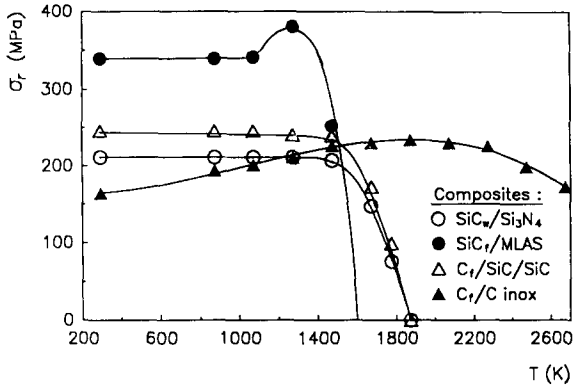

Fig. 15. Change in the rupture stress σ_r as a function of temperature T for different CMCs (f fibers, w whiskers). From Jamet [12].

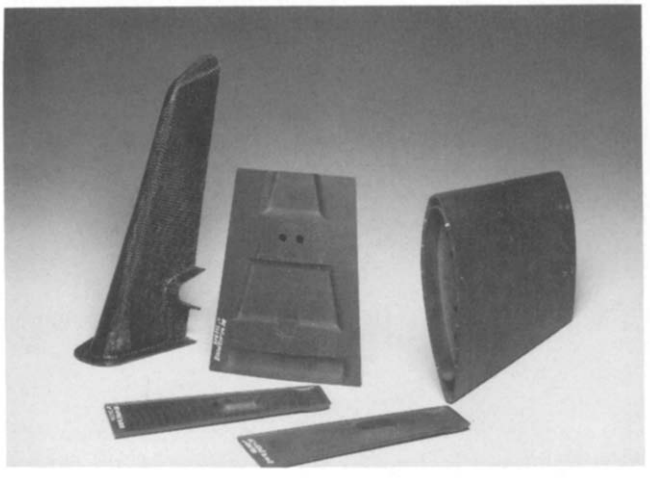

Fig. 16. Different parts made of carbon–silicon-carbide and silicon-carbide–silicon-carbide for aircraft industry (SEP).

aircraft engines—tubes for ramjets, exhaust cones, flame holder rings, casing struts, cold and hot nozzle flaps (Fig. 16); the nozzle flaps are now in use on the Mirage 2000 and the Rafale (cold flaps of C_f–SiC and hot flaps of SiC_f–SiC from SEP);
rocket motors—various combustion chambers for liquid bipropellant engines, nozzles and other components for solid-fuel motors, nozzle exit cones of C_f–SiC for Ariane;
aerospace structures—the Hermès shuttle is a prime example of the need which exists for thermostructural composites; many parts have now been developed, including nose, leading edges (Fig. 17), large panels (approximately 2 × 1 m^2), stabilizers, elevons.

7. Conclusion

Ceramic matrix composites are a new class of very promising materials with high potential for high temperature applications. Their mechanical behavior is

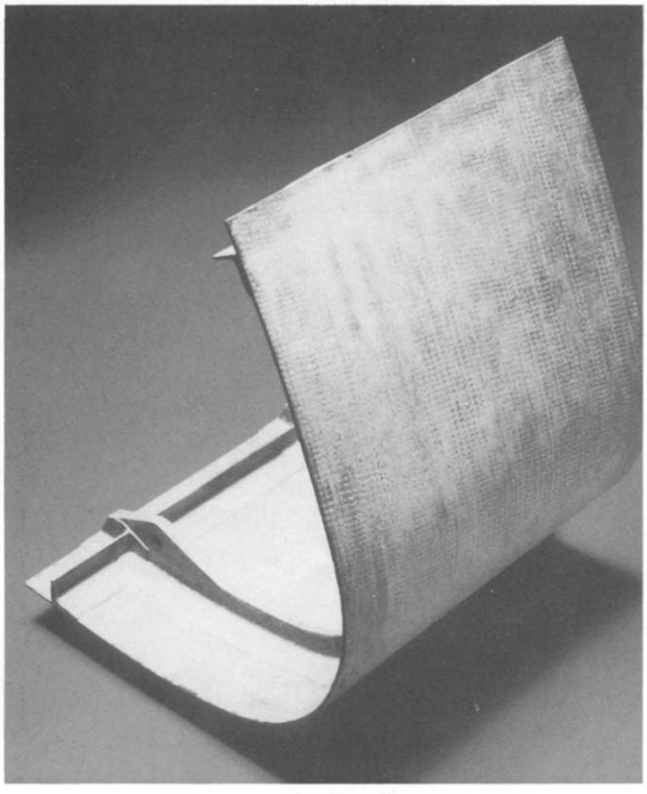

Fig. 17. Leading edge for Hermès shuttle in carbon–carbon protected against oxidation (Aérospatiale).

very specific and is governed by the interfaces between fibers and matrix and by the stability of the fibers during long temperature exposure. Their strength-to-weight ratio and temperature capability make CMCs the best candidates for the highest temperature uses.

Acknowledgments

The authors wish to thank Dr F. Albugues from Aérospatiale Company, Etablissement de Bordeaux, Dr F. Christin from SEP Company, Etablissement de Bordeaux, for their comments and help regarding the CMC applications. Thanks are also due to our colleagues for their results: Dr F. Abbé, Dr P. Fourvel, Mr D. Kervadec and Dr I. Lhermitte.

References

1 J. L. Chermant, *Céramiques Thermomécaniques*, Les Presses du CNRS, Paris, 1989.
2 R. J. Brook, in J. A. Pask and A. G. Evans (eds.), *Ceramic Microstructures '86—Role of Interfaces*, Materials Science Research, Plenum, NY, Vol. 21, 1987, p. 15.
3 A. G. Evans, in J. A. Pask and A. G. Evans (eds.), *Ceramic Microstructures '86—Role of Interfaces*, Materials Science Research, Plenum, NY, Vol. 21, 1987, p. 775.
4 R. Roy, in J. A. Pask and A. G. Evans (eds.), *Ceramic Microstructures '86—Role of Interfaces*, Materials Science Research, Vol. 21, 1987, p. 25.
5 M. Taya and R. J. Arsenault, *Metal Matrix Composites: Thermomechanical Behavior*, Pergamon, Oxford, 1989.
6 D. L. Anton, P. L. Martin, D. B. Miracle and R. McMeeking, *Intermetallic Matrix Composites*, Materials Research Society Proceedings, Materials Research Society, Pittsburgh, PA, Vol. 194, 1990.
7 A. G. Evans, *Mater. Sci. Eng., A143* (1991) 63.
8 J. Clark and M. Flemings, *Pour la Sci., 110* (1986) 18.
9 P. Langereux, *Air Cosmos, 1072* (1985) 39.
10 F. Christin, R. Naslain and C. Bernard, *Proc. 7th Int. Conf. on Chemical Vapor Deposition*, The Electrochemical Society, Princeton, NJ, 1979, p. 499.
11 R. Naslain, *Introduction aux Matériaux Composites: 2, Matrices Métalliques et Céramiques*, éditions du CNRS and Institut des Matériaux Composites, Bordeaux, France, 1985.
12 J. F. Jamet, in Dunod (ed.), *Science et Défense 90, Les Nouveaux Matériaux*, Dunod, Paris, 1990, p. 93.
13 M. Coster and J. L. Chermant, *Précis d'Analyse d'Images, Les Editions du CNRS, 1985*, Les Presses du CNRS, Paris, 1989, 2nd edn.
14 F. Abbé, L. Chermant, M. Coster, M. Gomina and J. L. Chermant, *Comp. Sci. Technol. 37* (1990) 109.
15 J. Serra, *Image Analysis and Mathematical Morphology*, Academic Press, New York, 1982.
16 F. Abbé and J. L. Chermant, *Acta Stereol., 8* (1989) 243.
17 J. L. Chermant, in Lattice Defects in Ceramics, *Jpn. J. Appl. Phys., Ser. 2* (1989) 179.
18 H. Osmani, D. Rouby, G. Fantozzi and J. M. Lequertier, *Comp. Sci. Technol., 37* (1990) 191.
19 P. Lamidieu and C. Gault, *Rev. Phys. Appl., 23* (1988) 201.
20 M. Gomina, *Thèse de Doctorat d'Etat*, Université de Caen, 1987.
21 M. Gomina, F. Abbé, P. Fourvel, M. H. Rouillon, J. Vicens and J. L. Chermant, in Lattice Defects in Ceramics, *Jpn. J. Appl. Phys., Ser. 2* (1989) 75.
22 N. Frety and M. Boussuge, *Comp. Sci. Technol., 37* (1990) 177.
23 J. J. Choury, Thermostructural composite materials in aeronautics and space applications, in *French Aerospace 1989 Aeronautical and Space Conf., Delhi, India, February 15–17, 1989, and Bangalore, India, February 20–22, 1989.*
24 J. R. Rice, *J. Appl. Mech. Trans. ASME*, (1968) 379.
25 S. J. Garwood, J. N. Robinson and C. E. Turner, *Int. J. Fract., 11* (1975) 528.
26 S. J. Garwood and C. E. Turner, *Fracture, Int. Congress of Fracture 4, Waterloo, Canada, June 19–24, 1977*, Vol. 3, University of Waterloo Press, 1977, p. 279.
27 M. Sakai, K. Urashima and M. Inagaki, *J. Am. Ceram. Soc., 66* (1983) 868.
28 M. Sakai and R. C. Bradt, in R. C. Bradt, A. G. Evans, D. P. H. Hasselman and F. F. Lange (eds.), *Fracture Mechanics of Ceramics*, Vol. 7, Plenum, New York, 1986, p. 127.
29 M. Gomina, J. L. Chermant and F. Osterstock, in P. Lamicq, W. T. G. Bunk and J. G. Wurm (eds.), *Advanced Materials Research and Developments for Transport—Composites, Strasbourg, November 26–28, 1985*, p. 117.
30 P. Fourvel, M. Gomina and J. L. Chermant, in R. Naslain, J. Lamalle and J. L. Zulian (eds.), *Materiaux Composites pour Applications à Hautes Températures, Coll. AMAC-CODEMAC, Bordeaux, March 29–30, 1990*, AMAC-CODEMAC, Bordeaux, France, 1990, p. 153.
31 G. Bernhardt, P. Lamicq and P. Macé, *Ind. Céram., 790* (1985) 51.
32 F. Abbé and J. L. Chermant, *Fourth Int. Conf. on Creep and Fracture of Engineering Materials and Structures, Swansea,*

April 1–6, 1990, The Institute of Metals, London, 1990, p. 439.
33 J. W. Holmes, *J. Mater. Sci.*, *26* (1991) 1808.
34 M. Gomina, J. L. Chermant and P. Fourvel, in *Fracture Mechanics of Ceramics, Nagoya, July 15–17, 1991*, in the press.
35 D. Kervadec and J. L. Chermant, in *Fracture Mechanics of Ceramics, Nagoya, July 15–17, 1991*, in the press.
36 P. Lamicq, in Dunod (ed.), *Sciences et Défense 90, Les Nouveaux Matériaux*, 1990, p. 93.
37 P. Peres, L. Anquez and J. F. Jamet, *Rev. Phys. Appl.*, *23* (1988) 213.
38 D. B. Marshall, *J. Am. Ceram. Soc.*, *67* (1984) C259.
39 P. D. Jero and R. J. Kerans, *Scripta Met. Mater.*, *24* (1990) 2315.
40 R. J. Kerans, R. S. Hay and N. J. Pagano, *Am. Ceram. Bull.*, *68* (1989) 429.
41 E. Y. Luh and A. G. Evans, *J. Am. Ceram. Soc.*, *70* (1987) 466.
42 D. Thouless, O. Sbaizero, L. Sigl and A. G. Evans, *J. Am. Ceram. Soc.*, *72* (1989) 525.
43 A. G. Evans and D. B. Marshall, *Acta Metall.*, *37* (1989) 2567.
44 H. S. Tsai, A. M. Arocho and L. W. Gause, *Mater. Sci. Eng.*, *A126* (1990) 295.
45 A. G. Evans, M. C. Lu, S. Schmauder and M. Rühle, *Acta Metall.*, *34* (1986) 1643.
46 M. D. Thouless and A. G. Evans, *Acta Metall.*, *36* (1988) 517.
47 J. J. Brennan, *Mater. Sci. Eng.*, *A126* (1990) 203.
48 B. N. Cox, *Acta Met. Mater.*, *39* (1991) 1189.
49 X. Z. Hu, E. H. Lutz and M. V. Swain, *J. Am. Ceram. Soc.*, *74* (1991) 1828.
50 C. H. Hsueh, *J. Mater. Sci.*, *25* (1990) 811, 818.
51 T. Kishi, M. Enoki and H. Tsuda, *Mater. Sci. Eng. A143* (1991) 103.
52 M. Monthioux, D. Cojean, O. Delverdier and P. Le Costumer, *Microsc. Microanal. Microstruct.*, *2* (1991) 47.
53 N. E. Paton, *Mater. Sci. Eng.*, *A143* (1991) 21.
54 J. F. Janhet, *40th Congress of the International Astronautical Federation, Malaga, October 8–13, 1989.*
55 D. Kervadec and J. L. Chermant, *Rev. Comp. Nouv. Mater.*, *1* (1991) 9.